ERa inhibits the progression of hepatocellular carcinoma by regulating the circRNA/miRNA/SMADs network

Changfeng Liu[A–D,F], Zujian Wu[B,C,E,F], Bing Zhang[B,C,E,F], Zhi Chen[A,E,F]

Department of Hepatobiliary and Pancreatic Surgery, Tongde Hospital of Zhejiang Province, Hangzhou, China

A – research concept and design; B – collection and/or assembly of data; C – data analysis and interpretation;
D – writing the article; E – critical revision of the article; F – final approval of the article

Advances in Clinical and Experimental Medicine, ISSN 1899–5276 (print), ISSN 2451–2680 (online) *Adv Clin Exp Med*. 2026;35(1):65–76

Address for correspondence
Zhi Chen
E-mail: ZhiCHenn_n@outlook.com

Funding sources
This work was supported by grants from the Zhejiang Province medical and health science and technology project (grant No. 2022KY699) and Chinese Medicine Research Program of Zhejiang Province (grants No. 2022ZB080 and No. GZY-ZJ-KJ-24060).

Conflict of interest
None declared

Received on September 23, 2024
Reviewed on December 24, 2024
Accepted on March 24, 2025

Published online on January 5, 2026

Abstract

Background. Hepatocellular carcinoma (HCC) shows significant differences in incidence and mortality between genders.

Objectives. This study investigates the mechanisms by which estrogen receptors (ER), specifically *ERa*, influence HCC outcomes.

Materials and methods. Bioinformatics approaches were used to study estrogen and its related pathways in relation to HCC. Estrogen receptor expression levels, along with downstream circular RNAs (circRNAs) and microRNAs (miRNAs), were measured in MHCC97H cells via quantitative reverse transcription polymerase chain reaction (RT-qPCR). Western blot was used to assess estrogen receptor 1 (*ESR1*) and SMAD family member 7 (*SMAD7*) protein expression. Cell proliferation, migration and cell cycle status of MHCC97H cells were measured using Cell Counting Kit-8 (CCK-8), Transwell assays and flow cytometry for cell cycle analysis.

Results. Bioinformatics analysis revealed that *ERa* acts as a transcription factor (TF) for 9 circRNAs with differential expression in HCC. We constructed the *ERa*/circRNA/miRNA/SMADs network based on the downstream targets of circRNAs, which were associated with the SMADs family. Survival studies revealed that *ESR1* is correlated with favorable patient survival in liver cancer. In MHCC97H cells, qRT-PCR findings showed low expression of *ESR1*, hsa_circ_0004913 and *SMAD7*, but significant expression of hsa-miR-96-5p. Overexpression of *ESR1* significantly increased the expression of hsa_circ_0004913 and *SMAD7* while suppressing hsa-miR-96-5p. Western blot analysis confirmed these findings. Furthermore, *ESR1* overexpression reduced MHCC97H cell proliferation and migration while inhibiting growth through G1 phase arrest. *ESR1* acts as a TF that binds to the promoter of hsa_circ_0004913, as demonstrated using chromatin Immunoprecipitation followed by chromatin immunoprecipitation-quantitative real-time PCR (ChIP-qPCR). A dual-luciferase reporter experiment confirmed that hsa_circ_0004913 targets and regulates hsa-miR-96-5p.

Conclusions. *ERa* can function as aTF, modulating the expression of various circRNAs with differential expression in HCC. Through this regulation, it modulates the circRNA/miRNA/SMADs network, thereby inhibiting the progression of HCC.

Key words: hepatocellular carcinoma, ceRNA network, transcription factor, estrogen receptor alpha, circular RNAs

Cite as
Liu C, Wu Z, Zhang B, Chen Z. *ERa* inhibits the progression of hepatocellular carcinoma by regulating the circRNA/miRNA/SMADs network. *Adv Clin Exp Med*. 2026;35(1):65–76. doi:10.17219/acem/203285

DOI
10.17219/acem/203285

Highlights

- *ERα* drives circRNA expression in hepatocellular carcinoma (HCC): Estrogen receptor α controls key differentially expressed circular RNAs, revealing new epigenetic regulators in HCC.
- *ESR1* overexpression inhibits HCC cell growth: Restoring *ESR1* function in MHCC97H liver cancer cells significantly reduces proliferation and migration.
- *ERα* modulates the circRNA/miRNA/SMAD signaling axis: This hormone receptor-driven network suppresses HCC development by coordinating noncoding RNA and SMAD pathways.
- hsa_circ_0004913 directly targets hsa-miR-96-5p: Dual-luciferase reporter assays validate this circRNA–miRNA interaction, highlighting a promising therapeutic target.

Background

Liver cancer was the 6th most common cancer worldwide in 2022 and the 3rd leading cause of cancer-related deaths, with hepatocellular carcinoma (HCC) accounting for 75–85% of cases.[1] The prognosis of HCC is closely associated with the stage of the disease. While advancements in targeted immunotherapy have improved survival rates in recent years, 2023 cancer statistics indicate that the 5-year survival rate for HCC remains low. Specifically, it is approx. 36% for early-stage cases and only 13% for advanced metastatic cases.[2] Furthermore, HCC ranks as the 2nd leading cause of cancer mortality among men. In most regions globally, the incidence and mortality rates of HCC are 2–3 times higher in men than in women.[1] Research has shown that the duration of estrogen exposure and the age at which HCC first appears are positively correlated, with a notable increase in HCC incidence observed among postmenopausal women.[3] Research by O'Brien et al. revealed a significant rise in HCC prevalence in female mice following ovariectomy. Additionally, female mice with knockout *ESR1* genes, which encode the estrogen receptor alpha (*ERα*), exhibited a 9-fold increase in HCC incidence. In contrast, the absence of the *ESR2* gene, encoding the estrogen receptor beta (*ERβ*), did not influence HCC development.[4] These findings suggest that the estrogen signaling pathway, mediated by *ERα*, could be a crucial target for HCC therapy. However, the exact mechanisms remain unclear, highlighting the need for further investigation into the role and regulatory pathways of the estrogen signaling system in HCC.

The circular RNAs (circRNAs) are evolutionarily conserved non-coding RNAs that form circular structures without 3' or 5' ends.[5] The unique closed-loop conformation of circRNAs imparts a higher degree of stability compared to most linear RNAs, and these molecules demonstrate significantly differential expression between malignant tissues and their adjacent non-malignant counterparts.[1] Unbalanced circRNA expression has been found as a possible biomarker for HCC diagnosis and treatment targeting.[6,7] Recent studies have shown that circRNAs can act as "gene sponges" for miRNAs, indirectly influencing the expression of miRNA target genes through competitive binding interactions.[8] MiRNAs are key regulators of gene expression at the post-transcriptional level, exerting their effects by base pairing with target sequences in the 3'UTR of messenger RNAs. They play an integral role in the pathogenesis of liver cancer.[9,10] Nevertheless, although these studies have elucidated the downstream regulatory mechanisms of circRNAs, the upstream regulatory mechanisms and the factors regulating circRNAs expression remain unclear. Wang et al. demonstrated that circCCDC66 was significantly elevated in non-small cell lung cancer, with *STAT3* directly interacting with the circCCDC66 promoter to enhance its transcriptional activity.[11] Our preliminary bioinformatics analysis suggests that *ERα* may serve as a transcription factor (TF) for several circRNAs that are differentially expressed in HCC tissues.

Objectives

Based on the above findings, we hypothesized that *ERα*, acting as a, regulates the production of circRNAs associated with HCC, thereby influencing its progression. The SMAD family plays an important role in the transition from liver fibrosis to HCC and has emerged as a prominent area of emphasis in liver cancer research.[12]

We employed bioinformatics methodologies to construct the *ERα*/circRNA/miRNA/SMADs network. A substantial body of evidence suggests that several coding and non-coding RNAs within this network, including hsa_circ_0004913, hsa-miR-96-5p and SMAD proteins, are involved in the development of HCC.[12–16]

SMAD7 acts as a suppressive element in HCC. A Kaplan–Meier analysis of HCC patients indicated that higher expression levels of *SMAD7* were associated with longer survival durations.[17] Moreover, previous research has shown that hsa-miR-96-5p may inhibit *SMAD7* expression through target regulation.[18,19] Consequently, the present study focuses on the *ERα*/hsa_circ_0004913/hsa-miR-96-5p/SMAD7 axis, aiming to elucidate the mechanisms

by which *ERα*, as a TF for circular RNAs (circRNAs), regulates the *ERα*/circRNA/miRNA/SMADs network to inhibit HCC progression.

Materials and methods

Ethics approval and consent to participate

Our study is based on publicly available data from open-source databases. The Tongde Hospital of Zhejiang Province (Hangzhou, China) does not require ethics committee review for research utilizing publicly available data. As a result, our study does not raise any ethical concerns or conflicts of interest.

Bioinformatics analysis

The Hepatocellular Carcinoma Database (HCCDB; http://lifeome.net/database/hccdb/home.html) was used to investigate the expression of *ESR1* in liver tumors and neighboring normal tissues, as well as in normal liver tissues. The Cancer Genome Atlas (TCGA; https://portal.gdc.cancer.gov) database was utilized to compare the difference in overall survival (OS) between HCC patients in various expression groups. The circRNA expression data for HCC were retrieved from the Gene Expression Omnibus (GEO) database (https://www.ncbi.nlm.nih.gov/geo) using the keywords "circRNA" and "hepatocellular carcinoma". Furthermore, the circRNA names were standardized according to the circBase database (http://www.circbase.org). All GEO data sets were analyzed using R v. 4.2.2 (R Foundation for Statistical Computing, Vienna, Austria) and the limma package. Only circRNAs with a log2 > 2 and $p < 0.05$ were selected. The circRNA promoter sequence was retrieved from the University of California Santa Cruz (UCSC) database (http://genome.ucsc.edu). To anticipate possible TFs, we utilized the JASPAR database (http://jaspar.genereg.net). The target miRNAs of the circRNA were predicted using the online tool circBank (https://www.circbank.cn/#/home). The target miRNAs of the circRNA were predicted using the online tool CircNetVis (https://www.meb.ki.se/shiny/truvu/CircNetVis/), retaining only the intersection of the prediction results from the Miranda and TargetScan databases for further analysis. Only those predicted by at least 2 of the databases to have potential regulatory effects were included in the study.

Cell culture and transfection

The Chinese Academy of Sciences Cell Bank (Shanghai, China) provided the human HCC cells (MHCC97H). The cells were grown at 37°C in a humidified atmosphere with 5% CO_2 and were maintained in Dulbecco's modified Eagle's medium (DMEM) supplemented with 10% fetal bovine serum (FBS). *ESR1*-pcDNA3.1 plasmids and the corresponding control vectors were generated by Genecreate (Wuhan, China). MHCC97H cells were transfected using the Lipofectamine 2000 reagent (Invitrogen, Waltham, USA).

Total RNA preparation and RT-qPCR

Total RNA and miRNA were extracted from MHCC97H cells using the miRcute miRNA Isolation Kit (DP501; Tiangen, Beijing, China) following the manufacturer's instructions. Briefly, 1×10^5–10^7 cells were lysed with Lysis Buffer. RNA was transferred to miRspin columns and eluted after buffer washing. Reverse transcription was performed using the ReverTra Ace qPCR RT Kit (FSQ-101; Toyobo, Osaka, Japan) for mRNA and the miRNA 1st Strand cDNA Synthesis Kit (MR101-02; Vazyme, Nanjing, China) for miRNA. Quantitative reverse transcription polymerase chain reaction (RT-qPCR) was performed using SYBR®Green Real time PCR Master Mix (QPK-201; Toyobo) for mRNA and miRNA Universal SYBR qPCR Master Mix (MQ101-02; Vazyme) for miRNA, and Real-time PCR System (SLAN-48P; Hongshi, Shanghai, China). The relative expression levels of the target genes were determined using the $2^{\wedge-\Delta\Delta Ct}$ method. This method made it possible to compare the expression of the genes in relation to *GAPDH* (for mRNA) or *U6* (for miRNA), the internal control gene. To ensure the reproducibility and reliability of the RT-qPCR results, each sample was amplified 3 times. Table 1 lists the specific primer sequences used in this study.

Cell Counting Kit-8 assay

A total of 1,000 cells were seeded into each well of a 96-well plate and incubated in a 5% CO_2 incubator for 0, 24 and 48 h. Ten microliters of Cell Counting Kit-8 (CCK-8) solution (CCK-8 Cell Proliferation and Cytotoxicity Assay Kit, CA1210; Solarbio, Beijing, China) were added to each well, and the plates were incubated for an additional 30 min. After incubation, the absorbance was measured at approx. 450 nm using a microplate reader (MB-530; Heales, Shenzhen, China). The IC50 (half-maximal inhibitory concentration) values were calculated by fitting concentration-response curves using the 4-parameter method. The color intensity was found to be proportional to the number of viable cells, as living cells reduced the CCK-8 dye to a colored formazan product.

Transwell assay

Cells were trypsinized, resuspended in serum-free DMEM, and counted using a hemocytometer. A total of 1×10^4 MHCC97H cells were seeded in the upper chamber of a 24-well Transwell insert (Corning Company, Corning, USA), while the lower chamber was filled with DMEM containing 10% FBS. The Transwell insert was then incubated in a humidified atmosphere of 5%

Table 1. Primer sequences

Primer	Sequence (5'to3')
ESR1 F	TCCTGATGATTGGTCTCGTCTGG
ESR1 R	GGTTCCTGTCCAAGAGCAAGTTAG
hsa_circ_0004913 F	GCCTGGGTGAATGCCTTGC
hsa_circ_0004913 R	ACTGTTGTGTCTGCTGTGTGC
hsa-miR-96-5p F	ACACTCCAGCTGGGTTTGGCACTAGCACATT
hsa-miR-96-5p R	CTCAACTGGTGTCGTGGAGTCGGCAATTCAGTTGAGAGCAAAAA
SMAD7 F	AACCCCCATCACCTTAG
SMAD7 R	CTCGTCTTCTCCTCCCA
U6 F	GCTTCGGCAGCACATATACTAAAAT
U6 R	CGCTTCACGAATTTGCGTGTCAT
GAPDH F	ACAACAGCCTCAAGATCATCAGC
GAPDH R	GCCATCACGCCACAGTTTCC

CO_2 at 37°C for 24 h to allow cell migration. After incubation, the insert was removed, and the medium was aspirated. Cells were fixed with 4% paraformaldehyde for 15 min and subsequently stained with 0.1% crystal violet for 20 min to visualize migrated cells. The insert was then rinsed 3 times with phosphate-buffered saline (PBS) to remove the unbound stain. A cotton swab was used to gently remove non-migrated cells from the upper surface of the membrane. Finally, migrated cells on the lower surface of the membrane were imaged under a light microscope (DSY5000X, COIC, Chongqing, China).

Flow cytometry assay for the cell cycle

After collecting and fixing the cell suspension, 5 mL of cold 70% ethanol was added, and the mixture was then incubated at 4°C overnight. Following 2 washes with 5 mL of PBS, the cells were stained for 10 min with 50 μg/mL propidium iodide (PI). After passing the suspension through a 300-mesh filter, it was centrifuged for 5 min at 1,000 rpm. To remove any remaining PI, 5 mL of PBS was used to rinse the cells. Subsequently, the cells were reconstituted in 200 μL of PBS and subjected to analysis using a Beckman Coulter flow cytometer (Beckman Coulter, Brea, USA).

Luciferase reporter assay

Both wild-type (WT) and mutant (MT) sequences were generated to investigate the role of hsa_circ_0004913 in cellular biology. Several recombinant reporter constructs were created by inserting these sequences into the pGL3 reporter gene vector. These recombinant reporters were then co-transfected into 293T cells along with hsa-miR-96-5p. Luciferase activity was precisely assessed 48 h after transfection using a dual-luciferase detection kit and the dual-luciferase reporter assay method. An internal control was included using the Renilla luciferase expression vector pRLTK (Takara, Beijing, China).

Chromatin immunoprecipitation-quantitative real-time PCR (ChIP-qPCR)

Following a seeding of MHCC97H cells (3×10^6) on 100 mm dishes and treatment with 1% formaldehyde, 600 μL of radioimmunoprecipitation assay (RIPA) lysis solution was used to lyse the cells. The sonicator was used to separate genomic DNA and shear it into 20–600-bp pieces. The chromatin was precipitated and incubated for an overnight duration at 4°C using either immunoglobulin G (IgG; Beyotime Biotechnology, Shanghai, China) or *ERα*-antibodies (Abcam, Shanghai, China) after centrifugation and removal of supernatants. The immune complexes were then cleaned using several washing buffers, including Tris-EDTA buffer, high salt, low salt, and LiCl. The immune precipitates were cross-linked overnight at 65°C after being eluted with 500 μL of elution buffer. hsa_circ_0004913 promoter primers were used to amplify *ESR1* binding sites. The promoter primers were as follow:

Primer 1:
forward (5'-ACTTCTCCCTCTGATACTCGTTCC-3'),
reverse (5'-ACTCCTCCTCCTTGATGCTGTAG-3');

Primer 2:
forward (5'-GGGAAGTGAGGACCCTAAGAAGC-3'),
reverse (5'-AAAAGCCCTGGAGCCAAGAAG-3');

Primer 3:
forward (5'-CGACTGACCGAGTATGGTATGG-3'),
reverse (5'-AGGAGGCAGGAAGTAGAGCGA-3').

Ultimately, DNA was extracted following the method recommended by the manufacturer, and RT-qPCR was used for analysis.

Western blot analysis

For immunoblotting, cells were lysed using preheated 2% sodium dodecyl sulfate (SDS) and then boiled for 30 min. Protein concentrations were determined using a bicinchoninic acid (BCA) assay (CW0014S; CoWin Biotech, Taizhou, China). Proteins were separated using SDS-polyacrylamide

gel electrophoresis (SDS-PAGE) and transferred to a nitrocellulose membrane (GE Healthcare, Chicago, USA) using the Genscript eBlot transfer technique. Membranes were blocked for 1 h at room temperature with 5% milk in 1× Tris-buffered saline with Tween-20 (TBST; 25 mM Tris, 150 mM NaCl, 2 mM KCl, pH 7.4, supplemented with 0.2% Tween-20) and probed overnight at 4°C with the indicated primary antibodies: *ERα* antibody (ab32063; Abcam) or *SMAD7* antibody (25840-1-AP; Proteintech, Wuhan, China). After washing with TBST 3 times for 30 min, membranes were incubated with peroxidase-conjugated secondary antibodies (SA00001-2; Proteintech) at room temperature for 1 h. The membranes were washed with TBST 3 times and detection was performed using Sensitive Chemiluminescence Test Kit (S6008M; UElany, Suzhou, China)

Statistical analyses

The normality assumption was assessed using the Shapiro–Wilk test, and the homogeneity of variance was evaluated with Levene's test. For data that met the test assumptions, differences between 2 groups were analyzed using the Student's t-test, and comparisons among multiple groups were performed using one-way analysis of variance (ANOVA). For small-sample data with a sample size below 7, the Mann–Whitney test was used for comparisons between 2 groups, and the Kruskal–Wallis test was applied for comparisons among multiple groups. Statistical significance was defined as $p < 0.05$. The corresponding results are provided in the shared data. The time from patient death or a 5-year follow-up is defined as the OS time. Kaplan–Meier method and log-rank test were used for survival analysis, and receiver operating characteristic (ROC) curve analysis was used to evaluate the discriminatory power of biomarkers. To evaluate heterogeneity among datasets, we used Cochran's Q test and the I^2 statistic. A fixed-effect model was applied when heterogeneity was minimal ($I^2 < 50\%$), assuming a consistent effect size across datasets. Conversely, a random-effects model was employed for analyses with substantial heterogeneity ($I^2 \geq 50\%$), accounting for between-study variability. Data analysis was performed using GraphPad Prism v. 7.0 (GraphPad Software, San Diego, USA), R v. 4.2.2 software (limma package v. 3.62.2; pheatmap package v. 1.0.12; survminer package v. 0.5.0) or IBM SPSS Statistics for Windows v. 24 (IBM Corp., Armonk, USA).

Results

ERα/circRNA/miRNA/*SMADs* network construction

CircRNA data from GSE97332 microarrays in the GEO database were analyzed using R v. 4.2.2. The top 30 differentially expressed circRNAs between cancer tissues and paired normal tissues were selected, including 15 with high expression and 15 with low expression. A heatmap was generated to display the hierarchical clustering of circRNA expression values (Fig. 1). The promoter sequence of circRNA was obtained from the UCSC database. The JASPAR database (https://jaspar.elixir.no) was used to predict potential TFs. ERα was the potential TF for 10 of these differentially expressed circRNA (Fig. 2).

The target miRNAs of circRNA were predicted using the online tool circBank. In the miRwalk online tool, predicted *SMADs* that overlap in at least 2 of the following databases–miRPathDB, miRWalk, and TargetScan–were considered, with a score greater than 0.95. Cytoscape was used to construct the *ERα*/circRNA/miRNA/*SMADs* network. We identified 8 circRNAs that were differentially expressed in HCC and ultimately target the *SMAD* family (Fig. 3).

Differential expression of the *ERα*/circRNA/miRNA/*SMADs* network is associated with poor prognosis in HCC

We used the HCCDB database to investigate *ESR1* expression in liver tumors and adjacent liver tissues, as well as in HCC and normal patient samples. Compared to the surrounding non-cancerous tissues, HCC tissues exhibited significantly lower *ESR1* expression (Fig. 4). Furthermore, *ESR1* expression was consistently lower in HCC

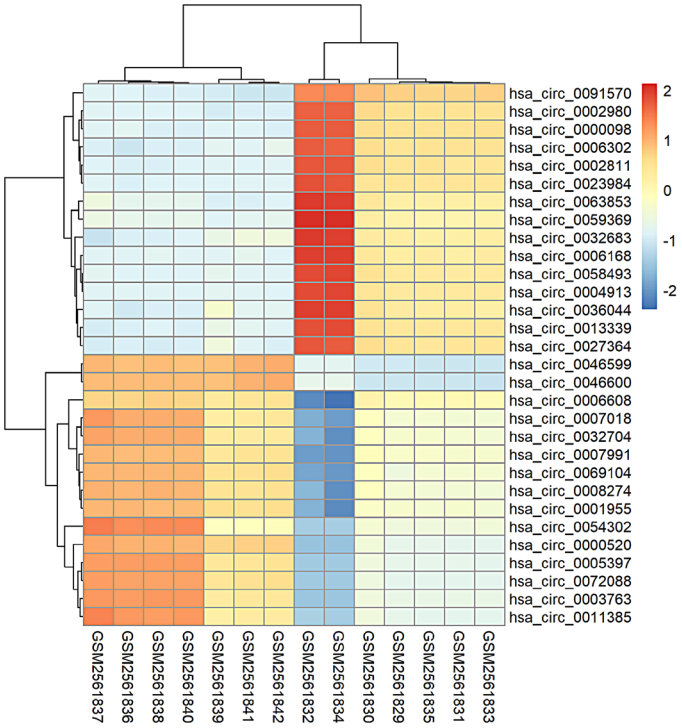

Fig. 1. Heatmap of 30 differentially expressed circular RNAs (circRNAs) in hepatocellular carcinoma (HCC). Differential expression analysis of circRNAs in the GSE97332 datasets was performed using the limma package. The top 30 differentially expressed circRNAs in HCC were selected, comprising 15 with high expression and 15 with low expression, based on a selection criterion of a log2 fold change ($|\log2FC| > 2$) and a $p < 0.05$. A heatmap illustrating these differential expression patterns was generated using the pheatmap package

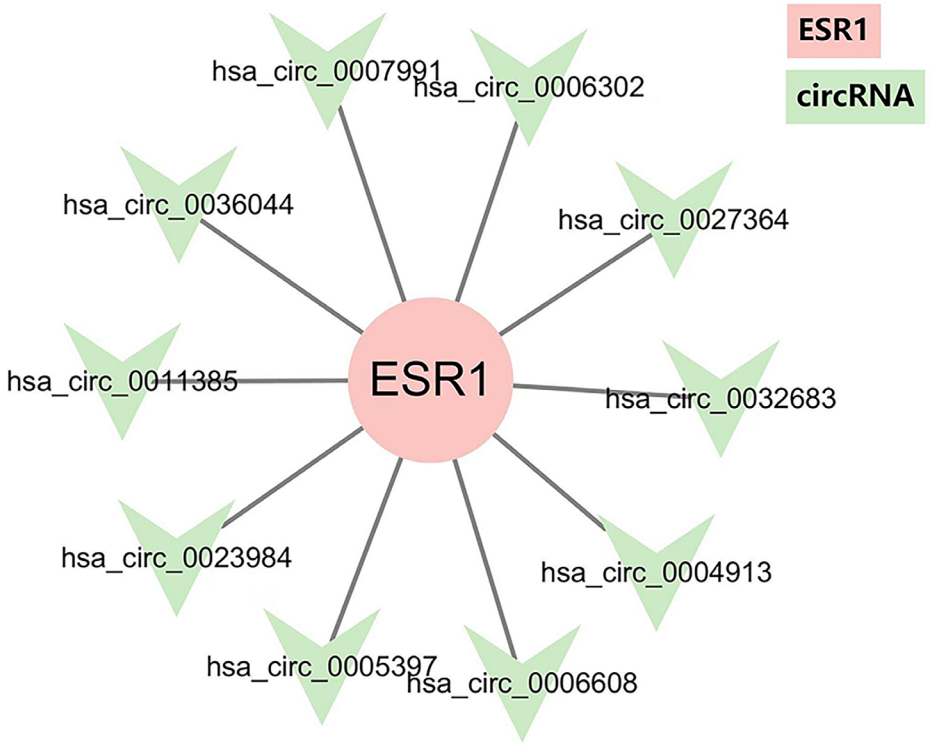

Fig. 2. Estrogen receptor alpha (*ERa*) is predicted as a transcription factor for 10 circular RNAs (circRNAs). Transcription factors of 30 differentially expressed circRNAs in hepatocellular carcinoma (HCC) were predicted using the JASPAR database. Among them, *ERa* was identified as a potential transcription factor for 10 circRNAs

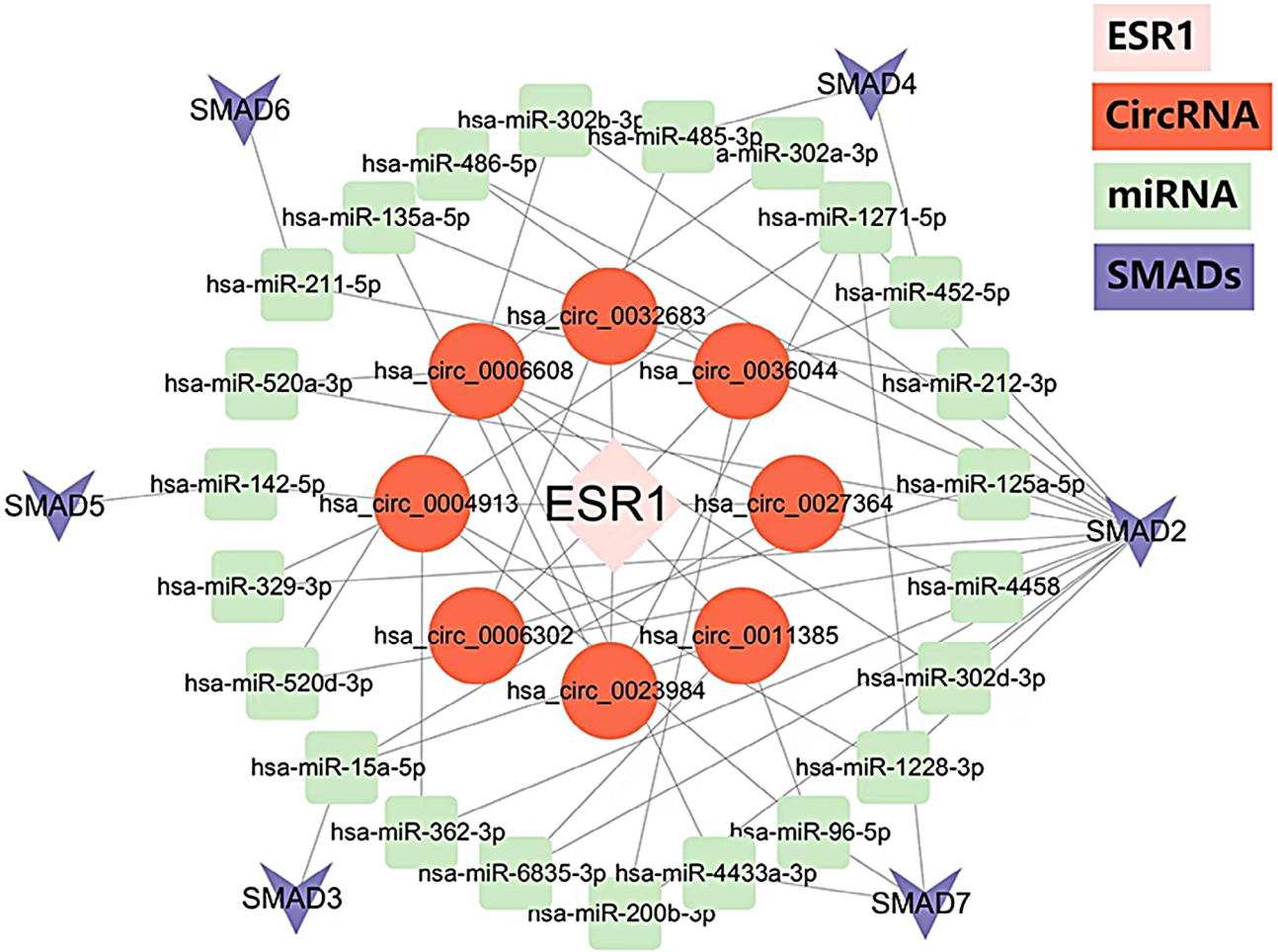

Fig. 3. Potential *ERa*/circRNA/miRNA/SMADs regulatory axis in hepatocellular carcinoma (HCC). Potential target miRNAs of circular RNAs (circRNAs) were predicted using the online tool circBank, while miRNA-targeted SMAD family genes were predicted using the online tool miRwalk. Ultimately, 8 circRNAs, 14 miRNAs and 4 genes from the SMAD family (*SMAD2*, *SMAD3*, *SMAD4*, *SMAD5*, *SMAD6*, and *SMAD7*) were identified, forming a potential *ERa*/circRNA/miRNA/SMADs regulatory axis in HCC

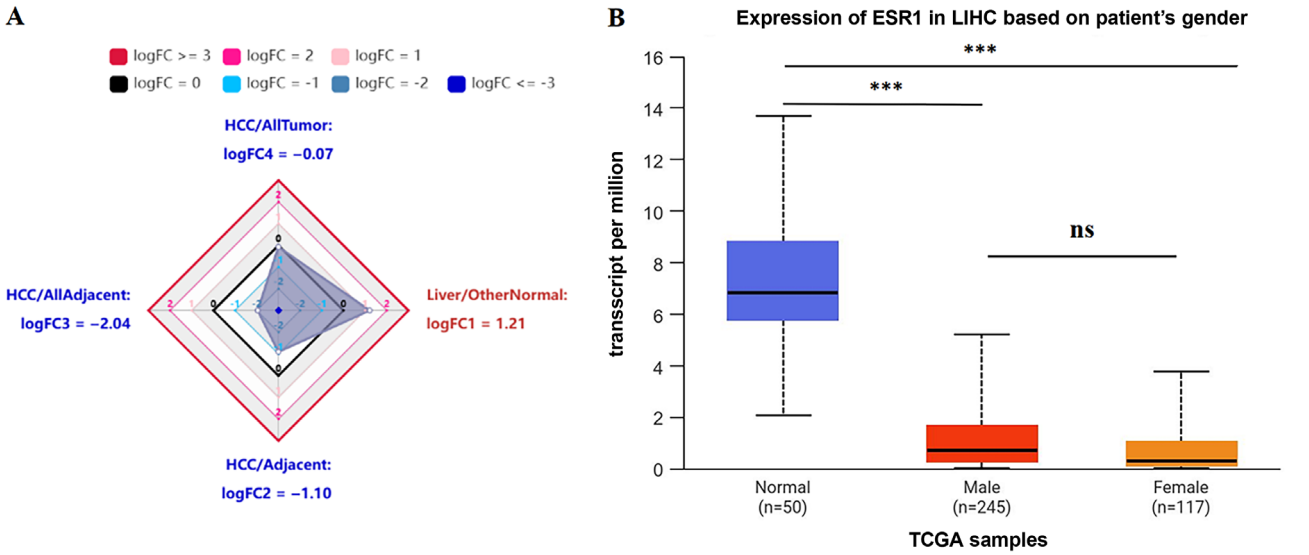

Fig. 4. *ESR1* expression in hepatocellular carcinoma (HCC) and adjacent tissues. A. Analysis of *ESR1* expression levels in HCC/All tumour, HCC/All Adjacent, HCC/Adjacent, and Liver/Other Normal tissues using the Hepatocellular Carcinoma Database (HCCDB) database. *ESR1* expression is significantly reduced in HCC tissues compared to adjacent non-cancerous tissues and healthy controls, regardless of gender, based on HCCDB analysis. Statistical significance is defined by |log2FC| > 1; B. Analysis of *ESR1* expression levels in liver tissues from 362 HCC patients (245 males and 117 females) and 50 normal individuals using The Cancer Genome Atlas (TCGA) data from the UALCAN website (https://ualcan.path.uab.edu). The results show that *ESR1* expression is significantly decreased in both male and female HCC patients compared to normal individuals ($p < 0.001$). However, there is no statistically significant difference in *ESR1* expression between male and female tumor patients ($p = 0.61$). Differences were analyzed using Welch's t-test and are presented as box plots showing the median and range

* $p < 0.05$; **$p < 0.01$; ***$p < 0.001$.

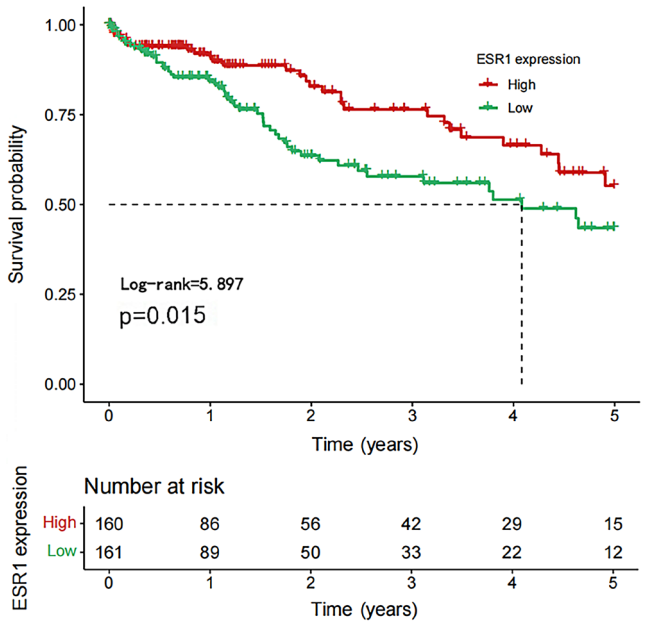

Fig. 5. Kaplan–Meier analysis shows that higher *ESR1* expression correlates with longer survival. Kaplan–Meier analysis and log-rank test were used to determine the relationship between *ESR1* expression and clinical prognosis in The Cancer Genome Atlas (TCGA) database. Overall survival (OS) time was defined as the time to patient death or the time of the last follow-up (up to 5 years). A total of 321 patients with non-zero OS were selected for the analysis, indicating a positive correlation between *ESR1* expression and OS in these patients ($p < 0.05$)

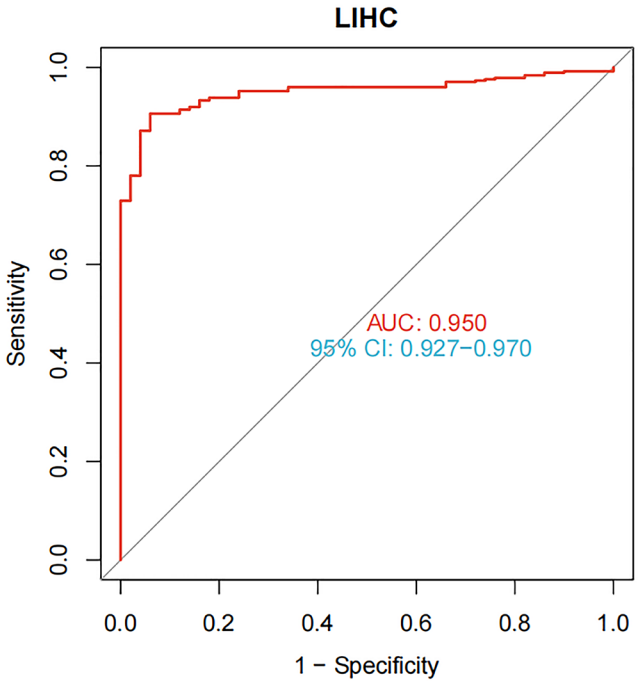

Fig. 6. Receiver operating characteristic (ROC) curve analysis showed that *ESR1* expression effectively distinguished tumor tissue from paired adjacent tissue, with an area under the curve (AUC) of 0.950 (95% confidence interval (95% CI): 0.927–0.970)

patients than in healthy individuals, regardless of gender (Fig. 4; $p < 0.001$). Based on our research, patients with high *ESR1* expression levels had significantly longer OS times compared to those with low expression levels (Fig. 5; $p = 0.015$). Additionally, ROC curve analysis demonstrated that *ESR1* expression effectively distinguished tumor tissue from paired adjacent tissue, with an area under the curve (AUC) of 0.950 (95% confidence interval (95% CI): 0.927–0.970; Fig. 6). The RT-qPCR results revealed that the liver

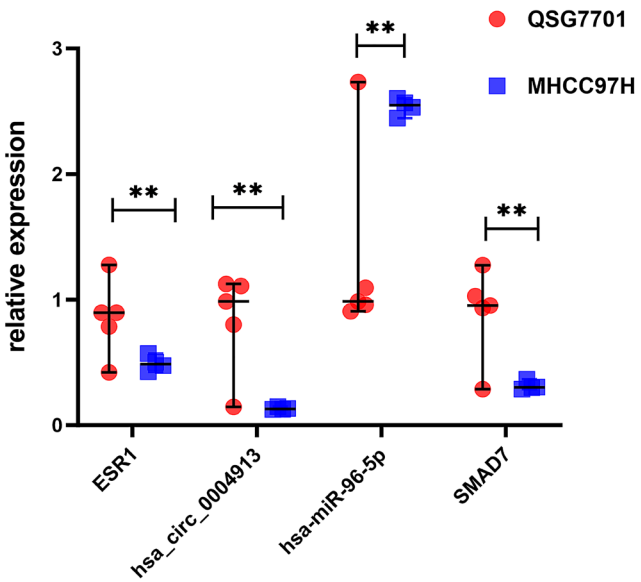

Fig. 7. Reverse transcription quantitative polymerase chain reaction (RT-qPCR) results between MHCC97H and QSG7701. RT-qPCR was performed to measure the expression levels of *ESR1*, hsa_circ_0004913, hsa-miR-96-5p, and *SMAD7* in the hepatocellular carcinoma (HCC) cell line MHCC97H and the normal liver cell line QSG7701. The results showed that, compared to normal QSG7701 liver cells, the MHCC97H liver cancer cells had higher levels of hsa-miR-96-5p, and lower levels of *ESR1*, hsa_circ_0004913 and *SMAD7*. Differences were analyzed using Mann–Whitney test and are expressed as median and range

* $p < 0.05$; ** $p < 0.01$; *** $p < 0.001$.

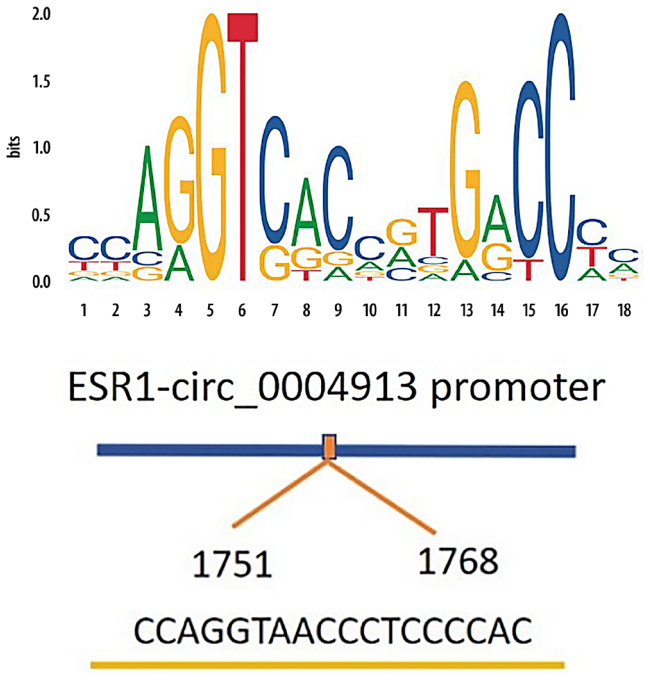

Fig. 8. Prediction of binding sites between *ESR1* and hsa_circ_0004913. Bioinformatics analyses predicted *ESR1* as a transcription factor for hsa_circ_0004913, with binding motifs identified using the JASPAR database

cancer cell line MHCC97H expressed higher levels of hsa-miR-96-5p and lower levels of *ESR1*, hsa_circ_0004913 and *SMAD7* compared to the normal control cell line QSG7701 (Fig. 7, $p = 0.008$). These findings suggest that a poor prognosis in HCC patients is associated with high expression of hsa-miR-96-5p and low expression of *ESR1* and *SMAD7*.

ERα promotes hsa_circ_0004913 expression in MHCC97H cells

To explore the upstream regulatory mechanisms of hsa_circ_0004913, we identified *ESR1* as a predicted TF using the JASPAR database. The JASPAR database was employed to predict the motif of *ESR1* (Fig. 8). Additionally, potential binding sites between *ERα* and the hsa_circ_0004913 promoter were predicted using the JASPAR database (Fig. 8). We used RT-qPCR to confirm that *ESR1* was overexpressed after plasmid transfection, and we found that there was a significant increase in hsa_circ_0004913 expression following *ESR1* overexpression (Supplementary Fig. 1). Additionally, ChIP-qPCR analysis revealed a strong binding affinity between the hsa_circ_0004913 promoter and *ESR1* at the sites targeted by the 3 primers (Fig. 9). Western blot analysis confirmed the successful extraction of protein samples with *GAPDH* as the internal control (Fig. 9). Collectively, these findings suggest that *ESR1* activates the transcription of hsa_circ_0004913, thereby enhancing its expression in MHCC97h cells.

ESR1 overexpression regulates the hsa_circ_0004913/hsa-miR-96-5p/*SMAD7* axis in MHCC97H

According to RT-qPCR data, *ESR1* overexpression significantly increased the expression of *SMAD7* while substantially decreasing the expression of hsa-miR-96-5p compared to the control group (Supplementary Fig. 2). Western blot analysis provided additional confirmation of these results (Supplementary Fig. 3). Hsa_circ_0004913 WT and MT sequences were created and transfected into 293T cells based on the anticipated binding sites (Supplementary Fig. 4). The results demonstrated that in the circ_0004913-WT group, the fluorescence of hsa-miR-96-5p mimics was significantly increased compared to negative control (NC) mimics ($p = 0.008$). Nevertheless, no significant difference in fluorescence was observed between NC mimics and hsa-miR-96-5p mimics in the circ_0004913-MT group (Supplementary Fig. 5). In summary, *ESR1* regulates the expression of the circRNA/miRNA/*SMADs* axis and hsa_circ_0004913 interacts with hsa-miR-96-5p in MHCC97H cells.

ESR1 overexpression suppresses the biological activity of MHCC97H cells

To investigate the biological effects of *ESR1* on MHCC97H cells, we transfected the cells with an *ESR1* plasmid and an empty vector, as well as with siRNAs targeting *ESR1* and a NC. Next, we evaluated MHCC97H

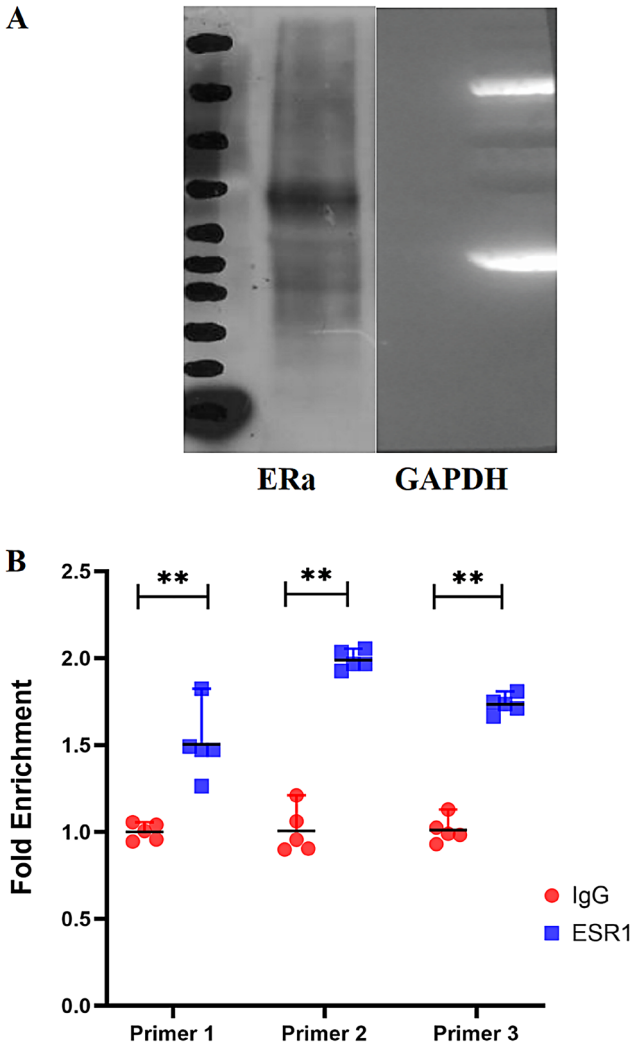

Fig. 9. Chromatin immunoprecipitation-quantitative real-time polymerase chain reaction (ChIP-qPCR) results. A. Western blot analysis showing *GAPDH* expression as an internal control for the estrogen receptor alpha (*ERα*) samples; B. The ChIP-qPCR experiment demonstrated that all 3 primers targeting the *ESR1* and hsa_circ_0004913 binding sites exhibited strong affinity, confirming the binding ability of *ESR1* to the hsa_circ_0004913 promoter. Differences were analyzed using Mann–Whitney test and are expressed as median and range

*p < 0.05; **p < 0.01; ***p < 0.001.

cells proliferation with the CCK-8 test, cell migration with the Transwell assay, and cell cycle distribution with flow cytometry. The results indicated that overexpression of *ESR1* significantly reduced cell proliferation, while silencing *ESR1* significantly enhanced cell proliferation ($p < 0.01$; Supplementary Fig. 6). The migratory capacity was much lower in the *ESR1* overexpression group than in the *ESR1* silencing group ($p < 0.01$; Supplementary Fig. 7). Furthermore, compared to the *ESR1* silencing group, the *ESR1* overexpression group showed an increase in the proportion of cells in the G1 phase, accompanied by a decrease in cells in the S and G2 phases. This suggests that *ESR1* inhibits tumor growth in MHCC97H cells by inducing G1 phase arrest (Supplementary Fig. 8; $p < 0.01$).

Discussion

The incidence and mortality of HCC vary significantly by gender.[1] In comparison to men, women had lower incidence and mortality rates from HCC. We found that, compared to normal liver tissues, HCC tissues exhibit a marked downregulation of *ESR1* expression, as confirmed with analysis of the TCGA database. Moreover, the concentration of *ESR1* in adjacent non-tumor tissues was significantly higher compared to that in HCC tissues. The results of the survival study showed a favorable association between the patient's survival times and *ESR1* levels. Kaplan–Meier analysis further demonstrated that higher *ESR1* expression was associated with longer survival in HCC patients. These findings suggest that the estrogen signaling pathway may play a protective role in HCC development and progression, offering a promising target for therapeutic intervention.

While substantial research has investigated the downstream regulatory mechanisms of circRNAs, their upstream regulatory pathways remain largely unexplored. Several studies have suggested that TFs can bind to circRNA promoter sequences, thereby regulating their expression.[20,21] Emerging evidence indicates that TFs, including *ERα*, can bind to circRNA promoter sequences, thereby modulating their transcriptional activity.

In this study, we analyzed differentially expressed circRNAs between adjacent non-tumor tissues and HCC using the GEO database and investigated potential TFs via the JASPAR database. We found that *ESR1* may function as a TF for multiple differentially expressed circular RNAs (circRNAs). Of these circRNAs, hsa_circ_0004913 was identified as a key regulator of the *ERα*/circRNA/miRNA/*SMADs* network.

Based on the "gene sponge" theory, we analyzed the potential miRNAs and mRNAs targeted by these circRNAs, constructing a circRNA-miRNA-mRNA network. This network comprises several pathways that converge on the *SMAD* family, primarily utilizing the *TGF-β/SMAD* signaling pathway to influence HCC development.[12,22] This network is closely associated with the *TGF-β/SMAD* signaling pathway, a critical driver in HCC pathogenesis. Several circRNAs and miRNAs within this network have been implicated in HCC initiation and progression through diverse mechanisms. For instance, hsa_circ_0058493 accelerates HCC progression by binding to *YTH* domain-containing protein 1.[23] Hsa_circ_0001955 acts as a miR-646 sponge, promoting angiogenesis in HCC.[24] MiR-200b-3p suppresses HCC cell growth by targeting *ERG* and *VEGF*-mediated angiogenesis.[25] MiR-329-3p enhances tumor cell responsiveness to T cell-induced cytotoxicity.[26] These findings suggest that this network is closely associated with the development of HCC and may be involved in various processes such as tumor angiogenesis, cellular activity, and immune sensitivity. Collectively, this network holds promise as a novel therapeutic target for HCC.

In this study, we hypothesize that *ESR1*, acting as a TF, differentially modulates the expression of specific circRNAs in HCC. This modulation influences the *SMADs* family expression and inhibits hepatocyte proliferation. The RT-qPCR analysis revealed that *ESR1* overexpression upregulates the expression of hsa_circ_0004913 and *SMAD7*, while downregulating hsa-miR-96-5p. Furthermore, ChIP-qPCR results confirmed that *ERα* interacts with the hsa_circ_0004913 promoter, enhancing its expression as a transcriptional regulator. Dual-luciferase reporter assays verified that hsa_circ_0004913 directly targets and regulates hsa-miR-96-5p. In vitro studies demonstrated that *ESR1* overexpression hinders HCC progression by inhibiting the proliferation and migration of MHCC97H cells, thereby inducing cell cycle arrest.

Many studies have also corroborated our findings. For instance, Li et al. conducted a study involving 150 HCC patients who underwent surgical treatment, with tissue specimens analyzed and clinical follow-up performed. The results indicated that the expression of hsa_circ_0004913 was significantly downregulated in liver cancer tissues compared to paired adjacent normal tissues. They reported significantly downregulated hsa_circ_0004913 in HCC tissues compared to adjacent normal tissues, correlating with shorter patient survival.[14]

Wu et al. demonstrated that hsa_circ_0004913 overexpression inhibits HCC progression by targeting miR-184, suppressing the *JAK2/STAT3/AKT* signaling pathway.[13] Additionally, hsa-miR-96-5p has been discovered to be significantly expressed in HCC, and its suppression can increase HCC apoptosis while reducing migration and invasion.[15,16]

Our study confirmed that hsa_circ_0004913 can target and regulate the expression of hsa-miR-96-5p. Similarly, Tang et al. demonstrated that in liver cancer cells, hsa-miR-96-5p is regulated by circ_0000972 through a gene-sponge mechanism, inhibiting HCC.[27] As mentioned earlier, several experiments have confirmed the targeting regulatory effect of hsa-miR-96-5p on *SMAD7*, which is consistent with our bioinformatics predictions.[18,19,28] Therefore, we did not perform further experimental validation. Besides *SMAD7*, *SMAD2*, *SMAD3*, and *SMAD4* are also potential targets within our predicted network, all of which belong to the *SMAD* family. Recent studies have demonstrated that the *SMAD* family mediates TF activation and the transmission of membrane-to-nucleus signals through the *TGF-β/SMAD* signaling pathway.[12] This pathway regulates multiple functions, including the tumor microenvironment, immune responses, tumor cell activity, and sensitivity to targeted therapies.[29–32] Additionally, it can crosstalk with other pathways, such as the *MAPK*, *PI3K/AKT* and *WNT/β*-catenin pathways, thereby amplifying its impact on tumor progression.[12] Thus, it plays a critical role in the initiation and progression of HCC.

In summary, the above indicates that the *ERα*/circRNA/miRNA/*SMADs* network may serve as a potential therapeutic target for HCC.

Limitations

Our study has several limitations. Our primary focus was on the gender differences in the incidence and mortality of HCC. Our analyses identified ERα as a TF regulating multiple differentially expressed circRNAs in HCC. It also modulates the circRNA/miRNA/SMAD network to suppress HCC progression. However, our study does not explore the potential pathways involved, nor does it examine the diagnostic value of *ERα* and hsa_circ_0004913 in HCC. Additionally, the small sample size may limit the statistical significance of our findings. Future large-scale studies are necessary.

Conclusions

The *ERα* signaling pathway represents a potential therapeutic target for HCC. We propose that *ERα*, functioning as a TF, , regulates the production of circRNAs that are differentially expressed in HCC. This modulates the circRNA/miRNA/SMAD network and slows the progression of the cancer. We hope this research will contribute to securing additional funding for further studies aimed at improving the survival rates of HCC patients.

Supplementary data

The supplementary materials are available at https://doi.org/10.5281/zenodo.15004445. The package includes the following files:

Supplementary Fig. 1. qRT-PCR detection of the relationship between *ESR1* and hsa_circ_0004913 expression. qRT-PCR analysis validated the overexpression of *ESR1* in the MHCC97H cell line transfected with the *ESR1* plasmid (OE-*ESR1*), showing a significant increase compared to the pcDNA3.1 empty vector group (pcDNA3.1). Additionally, the overexpression of *ESR1* resulted in an upregulation of hsa_circ_0004913 expression. Differences were analyzed using Mann–Whitney test and are expressed as median and range (*$p < 0.05$, **$p < 0.01$, ***$p < 0.001$).

Supplementary Fig. 2. qRT-PCR detection of the relationship between *ESR1* hsa-miR-96-5p and SMAD7 expression. qRT-PCR data showed that overexpression of *ESR1* significantly increased the expression of *SMAD7*, while significantly decreased the expression of hsa-miR-96-5p. Differences were analyzed using Mann–Whitney test and are expressed as median and range (*$p < 0.05$, **$p < 0.01$, ***$p < 0.001$).

Supplementary Fig. 3. Western blot analysis confirmed that *ESR1* overexpression increases the expression level of *SMAD7*.

Supplementary Fig. 4. The target between hsa_circ_0004913 and hsa-miR- 96-5p were predicted through TargetScan.

Supplementary Fig. 5. Luciferase reporter assay revealed that in the circ-0004913-WT group, fluorescence

significantly increased in the hsa-miR-96-5p mimic group (miR-96-5p) compared to the NC mimics empty vector group (NC mimic) ($p < 0.05$), confirming the interaction and targeted regulation between hsa_circ_0004913 and hsa-miR-96-5p. Differences were analyzed using Mann–Whitney test and are expressed as median and range (*$p < 0.05$, **$p < 0.01$,***$p < 0.001$).

Supplementary Fig. 6. CCK-8 assay showed that overexpression of *ESR1* (OE-*ESR1*) reduced MHCC97H cell proliferation, while silencing of *ESR1* (si-*ESR1*) enhanced proliferation. Differences were analyzed using Mann–Whitney test and are expressed as median and range (*$p < 0.05$, **$p < 0.01$,***$p < 0.001$).

Supplementary Fig. 7. Transwell assay demonstrating that *ESR1* overexpression decreased cell migration, while silencing *ESR1* had the opposite effect. Differences were analyzed using Mann–Whitney test and are expressed as median and range (*$p < 0.05$, **$p < 0.01$,***$p < 0.001$).

Supplementary Fig. 8. Results of cell cycle. Compared to the *ESR1* silencing group, the *ESR1* overexpression group showed an increased proportion of cells in the G1 phase and a decreased proportion in the S and G2 phases. This suggests that *ESR1* inhibits tumor growth in MHCC97H cells by inducing G1 phase arrest. Differences were analyzed using Mann–Whitney test and are expressed as median and range (*$p < 0.05$, **$p < 0.01$,***$p < 0.001$).

Data Availability Statement

The datasets used and/or analyzed during the current study were obtained from publicly available sources, including from the HCCDB, TCGA, GEO, circBase, UCSC, and JASPAR.

Consent for publication

Not applicable.

Use of AI and AI-assisted technologies

Not applicable.

ORCID iDs

Changfeng Liu https://orcid.org/0000-0002-5129-127X
Zujian Wu https://orcid.org/0009-0005-7064-1895
Bing Zhang https://orcid.org/0009-0005-7018-054X
Zhi Chen https://orcid.org/0009-0002-1829-7861

References

1. Bray F, Laversanne M, Sung H, et al. Global cancer statistics 2022: GLOBOCAN estimates of incidence and mortality worldwide for 36 cancers in 185 countries. *CA Cancer J Clin*. 2024;74(3):229–263. doi:10.3322/caac.21834
2. Siegel RL, Miller KD, Wagle NS, Jemal A. Cancer statistics, 2023. *CA Cancer J Clin*. 2023;73(1):17–48. doi:10.3322/caac.21763
3. Hassan MM, Botrus G, Abdel-Wahab R, et al. Estrogen replacement reduces risk and increases survival times of women with hepatocellular carcinoma. *Clin Gastroenterol Hepatol*. 2017;15(11):1791–1799. doi:10.1016/j.cgh.2017.05.036
4. O'Brien MH, Pitot HC, Chung SH, Lambert PF, Drinkwater NR, Bilger A. Estrogen receptor-α suppresses liver carcinogenesis and establishes sex-specific gene expression. *Cancers (Basel)*. 2021;13(10):2355. doi:10.3390/cancers13102355
5. Mumtaz PT, Taban Q, Dar MA, et al. Deep insights in circular RNAs: From biogenesis to therapeutics. *Biol Proced Online*. 2020;22(1):10. doi:10.1186/s12575-020-00122-8
6. Hu Z, Chen G, Zhao Y, et al. Exosome-derived circCCAR1 promotes $CD8^+$ T-cell dysfunction and anti-PD1 resistance in hepatocellular carcinoma. *Mol Cancer*. 2023;22(1):55. doi:10.1186/s12943-023-01759-1
7. Zhou Y, Mao X, Peng R, Bai D. CircRNAs in hepatocellular carcinoma: Characteristic, functions and clinical significance. *Int J Med Sci*. 2022;19(14):2033–2043. doi:10.7150/ijms.74713
8. Zhao X, Zhong Y, Wang X, Shen J, An W. Advances in circular RNA and its applications. *Int J Med Sci*. 2022;19(6):975–985. doi:10.7150/ijms.71840
9. Hajizadeh M, Hajizadeh F, Ghaffarei S, et al. MicroRNAs and their vital role in apoptosis in hepatocellular carcinoma: MiRNA-based diagnostic and treatment methods. *Gene*. 2023;888:147803. doi:10.1016/j.gene.2023.147803
10. El-Mahdy HA, Sallam AAM, Ismail A, Elkhawaga SY, Elrebehy MA, Doghish AS. miRNAs inspirations in hepatocellular carcinoma: Detrimental and favorable aspects of key performers. *Pathol Res Pract*. 2022;233:153886. doi:10.1016/j.prp.2022.153886
11. Wang Y, Zhao W, Zhang S. STAT3-induced upregulation of circCCDC66 facilitates the progression of non-small cell lung cancer by targeting miR-33a-5p/KPNA4 axis. *Biomed Pharmacother*. 2020;126:110019. doi:10.1016/j.biopha.2020.110019
12. Xin X, Cheng X, Zeng F, Xu Q, Hou L. The role of TGF-β/SMAD signaling in hepatocellular carcinoma: From mechanism to therapy and prognosis. *Int J Biol Sci*. 2024;20(4):1436–1451. doi:10.7150/ijbs.89568
13. Wu M, Sun T, Xing L. Circ_0004913 inhibits cell growth, metastasis, and glycolysis by absorbing miR-184 to regulate *HAMP* in hepatocellular carcinoma. *Cancer Biother Radiopharm*. 2023;38(10):708–719. doi:10.1089/cbr.2020.3779
14. Li X, Yang J, Yang X, Cao T. Dysregulated circ_0004913, circ_0008160, circ_0000517, and their potential as biomarkers for disease monitoring and prognosis in hepatocellular carcinoma. *Clin Lab Anal*. 2021;35(6):e23785. doi:10.1002/jcla.23785
15. Yuan F, Tang Y, Cao M, et al. Identification of the hsa_circ_0039466/miR-96-5p/FOXO1 regulatory network in hepatocellular carcinoma by whole-transcriptome analysis. *Ann Transl Med*. 2022;10(14):769–769. doi:10.21037/atm-22-3147
16. Li ZR, Xu G, Zhu LY, Chen H, Zhu JM, Wu J. GPM6A expression is suppressed in hepatocellular carcinoma through miRNA-96 production. *Lab Invest*. 2022;102(11):1280–1291. doi:10.1038/s41374-022-00818-3
17. Feng T, Dzieran J, Gu X, et al. *SMAD7* regulates compensatory hepatocyte proliferation in damaged mouse liver and positively relates to better clinical outcome in human hepatocellular carcinoma. *Clin Sci (Lond)*. 2015;128(11):761–774. doi:10.1042/CS20140606
18. Gu H, Duan Y, Li S, et al. miR-96-5p regulates myocardial infarction-induced cardiac fibrosis via *SMAD7*/Smad3 pathway. *Acta Biochim Biophys Sin*. 2022;54(12):1874–1888. doi:10.3724/abbs.2022175
19. Kang J, Li Y, Zou Y, Zhao Z, Jiao L, Zhang H. miR-96-5p induces orbital fibroblasts differentiation by targeting *SMAD7* and promotes the development of thyroid-associated ophthalmopathy. *Evid Based Complement Alternat Med*. 2022;2022:8550307. doi:10.1155/2022/8550307
20. Zhou H, Huang J, Wang F. Increased transcription of hsa_circ_0000644 upon RUNX family transcription factor 3 downregulation participates in the malignant development of bladder cancer. *Cell Signal*. 2023;104:110590. doi:10.1016/j.cellsig.2023.110590
21. Ren L, Jiang M, Xue D, et al. Nitroxoline suppresses metastasis in bladder cancer via EGR1/circNDRG1/miR-520h/*SMAD7*/EMT signaling pathway. *Int J Biol Sci*. 2022;18(13):5207–5220. doi:10.7150/ijbs.69373
22. Zaidi S, Gough NR, Mishra L. Mechanisms and clinical significance of TGF-β in hepatocellular cancer progression. *Adv Cancer Res*. 2022;156:227–248. doi:10.1016/bs.acr.2022.02.002
23. Wu A, Hu Y, Xu Y, et al. Methyltransferase-like 3-mediated m6A methylation of Hsa_circ_0058493 accelerates hepatocellular carcinoma progression by binding to YTH domain-containing protein 1. *Front Cell Dev Biol*. 2021;9:762588. doi:10.3389/fcell.2021.762588

24. Li X, Lv J, Hou L, Guo X. Circ_0001955 acts as a miR-646 sponge to promote the proliferation, metastasis and angiogenesis of hepatocellular carcinoma. *Dig Dis Sci*. 2022;67(6):2257–2268. doi:10.1007/s10620-021-07053-8
25. Wang Y, Moh-Moh-Aung A, Wang T, et al. Exosomal delivery of miR-200b-3p suppresses the growth of hepatocellular carcinoma cells by targeting ERG- and VEGF-mediated angiogenesis. *Gene*. 2024; 931:148874. doi:10.1016/j.gene.2024.148874
26. Wang Y, Cao K. KDM1A promotes immunosuppression in hepatocellular carcinoma by regulating PD-L1 through demethylating MEF2D. *J Immunol Res*. 2021;2021:9965099. doi:10.1155/2021/9965099
27. Tang J, Tang R, Xue F, Gu P, Han J, Huang W. Circ_0000972 inhibits hepatocellular carcinoma cell stemness by targeting miR-96-5p/PFN1 [published online as ahead of print on December 2, 2024]. *Biochem Genet*. 2024. doi:10.1007/s10528-024-10975-3
28. Zhan J, Qi Y, Fu Y, et al. LncRNA ZFAS1 alleviated NLRP3 inflammasome-mediated pyroptosis through regulating miR-96-5p/*SMAD7* signaling in allergic rhinitis. *Int Arch Allergy Immunol*. 2024;185(7): 704–717. doi:10.1159/000535646
29. Gu J, Zhou J, Chen Q, et al. Tumor metabolite lactate promotes tumorigenesis by modulating MOESIN lactylation and enhancing TGF-β signaling in regulatory T cells. *Cell Rep*. 2022;39(12):110986. doi:10.1016/j.celrep.2022.110986
30. Bao W, Wang J, Fan K, Gao Y, Chen J. PIAS3 promotes ferroptosis by regulating TXNIP via TGF-β signaling pathway in hepatocellular carcinoma. *Pharmacol Res*. 2023;196:106915. doi:10.1016/j.phrs.2023.106915
31. Xin X, Li Z, Yan X, et al. Hepatocyte-specific Smad4 deficiency inhibits hepatocarcinogenesis by promoting CXCL10/CXCR3-dependent $CD8^+$-T cell-mediated anti-tumor immunity. *Theranostics*. 2024;14(15): 5853–5868. doi:10.7150/thno.97276
32. Ding J, Yang YY, Li PT, et al. TGF-β1/SMAD3-driven GLI2 isoform expression contributes to aggressive phenotypes of hepatocellular carcinoma. *Cancer Lett*. 2024;588:216768. doi:10.1016/j.canlet.2024.216768